Clim. Past Discuss., 11, 603–636, 2015
www.clim-past-discuss.net/11/603/2015/
doi:10.5194/cpd-11-603-2015

Climate of the Past
Discussions
Open Access

Modelled glacier equilibrium line altitudes during the mid-Holocene in the southern mid-latitudes

C. Bravo[1,2,3,*], M. Rojas[1,2,3], B. M. Anderson[4], A. N. Mackintosh[4], E. Sagredo[3,5], and P. I. Moreno[2,3,6]

[1]Department of Geophysics, Universidad de Chile, Santiago, Chile
[2]Center for Climate and Resilience Research (CR2), Universidad de Chile, Santiago, Chile
[3]Millenium Nucleus Paleoclimate of the Southern Hemisphere, Santiago, Chile
[4]Antarctic Research Centre, Victoria University of Wellington, Wellington, New Zealand
[5]Institute of Geography, Pontificia Universidad Católica de Chile, Santiago, Chile
[6]Department of Ecological Sciences and Institute of Ecology and Biodiversity, Universidad de Chile, Santiago, Chile
[*]now at: Glaciology Laboratory, Centro de Estudios Científicos, Valdivia, Chile

Received: 12 February 2015 – Accepted: 15 February 2015 – Published: 6 March 2015

Correspondence to: C. Bravo (claudio@dgf.uchile.cl)

Published by Copernicus Publications on behalf of the European Geosciences Union.

Abstract

Glacier behaviour during the mid-Holocene (MH, 6000 year BP) in the Southern Hemisphere provides observational data to constrain our understanding of the origin and propagation of palaeo-climatic signals. We examine the climatic forcing of glacier expansion in the MH by evaluating modelled glacier equilibrium line altitude (ELA) and climate conditions during the MH compared with pre-industrial time (PI, year 1750) in the mid latitudes of the Southern Hemisphere, specifically in Patagonia and the South Island of New Zealand. Climate conditions for the MH are obtained from PMIP2 models simulations, which in turn force a simple glacier mass balance model to simulate changes in equilibrium-line altitude during this period. Climate conditions during the MH show significantly ($p \leq 0.05$) colder temperatures in summer, autumn and winter, and significantly ($p \leq 0.05$) warmer temperatures in spring. These changes are a consequence of insolation differences between the two periods. Precipitation does not show significant changes, but exhibits a temporal pattern with less precipitation from August to September and more precipitation from October to April during the MH. In response to these climatic changes, glaciers in both analysed regions have an ELA that is 15–33 m lower than PI during the MH. The main causes of this difference are the colder temperature during the MH, reinforcing previous results that mid-latitude glaciers are more sensitive to temperature change compared to precipitation changes. Differences in temperature have a dual effect on mass balance. First, during summer and early autumn less energy is available for melting. Second in late autumn and winter, lower temperatures cause more precipitation to fall as snow rather than rain, resulting in more accumulation and higher surface albedo. For these reasons, we postulate that the modelled ELA changes, although small, may help to explain larger glacier extents observed in the mid Holocene in both South America and New Zealand.

CPD
11, 603–636, 2015

1 Introduction

Deciphering the climate signals and glacial history of the mid-latitudes of the Southern Hemisphere during the Holocene is key to unravelling the mechanism of climate change that occurred during this period. During the last ~ 11 500 years, a series of intervals of rapid climate changes occurred worldwide (Mayewski et al., 2004). Reduction in temperature and/or increases in precipitation during these periods have been recorded as multiple glacial advances in different areas of the planet. A recent global review of Holocene glacier activity is given in Solomina et al. (2015). These periods of renewed glacial activity, known as Neoglaciations (Porter and Denton, 1967), were initially identified in the Northern Hemisphere. However, during the last decades, numerous studies have shown evidence of glacial advances, as well as climate variability during this period in the Southern Hemisphere (approximately between 35 to 55° S). Most of these studies have focused on Patagonia (e.g. Clapperton and Sugden, 1988; Porter, 2000; Rodbell et al., 2009; Strelin et al., 2014) and in the Southern Alps in New Zealand (e.g. Gellatly et al., 1988; Porter, 2000; Schaefer et al., 2009; Putnam et al., 2012; Kaplan et al., 2013).

In Patagonia, a number of different Neoglacial chronologies have been produced (e.g. Mercer, 1982; Aniya, 1995, 2013; Clapperton and Sugden, 1988; Strelin et al., 2014). However, significant differences between these chronologies have not been fully resolved. The latest of these chronologies shows the largest advance occurring between 6000–5000 yr BP (Strelin et al., 2014).

In New Zealand, on the other hand, notable periods of glacier still stand or re-advance occurred during the early to mid-Holocene, as well as during the last millennium (Schaefer et al., 2009; Putnam et al., 2012). It appears that these decadal to centennial-scale glacier events have been superimposed on a long-term trend of decreasing ice extent that persisted for the entire Holocene (Schaefer et al., 2009; Putnam et al., 2012; Kaplan et al., 2013). Putnam et al. (2012) suggest that glacial advances

CPD
11, 603–636, 2015

in New Zealand were driven by the migration (southward shift) of the Inter-Tropical Convergence Zone (ITCZ).

In this context, it is clear that several aspects of the Neoglacial chronology of southern mid-latitudes (30–50° S) are still inadequately understood, and more high-resolution chronologies are needed. Particularly relevant for this study, is the lack of agreement regarding the timing of the onset of the Neoglaciations in the southern mid-latitudes (Porter, 2000).

Understanding the climate and glacial history of the southern mid-latitudes is a pre-requisite for testing hypothesis regarding the origin and propagation of palaeoclimate signals, the coupling of the ocean–atmosphere in the extra-tropics, and the interaction of low- and high-latitude climate controls on hemispheric and global climate (Fletcher and Moreno, 2012; Moreno et al., 2010; Rojas et al., 2009; Putnam et al., 2012). The mid-Holocene also represents a key moment in our late climate history, given that it corresponds to the period within the current interglacial cycle, with an important difference in orbital parameters with respect to the present conditions and devoid of influences from late-glacial climate change (Braconnot et al., 2007). These orbital differences result in an increase of incoming solar radiation at the top of the atmosphere in the Northern Hemisphere, and a decrease in the Southern Hemisphere (Braconnot et al., 2007). The southern mid-latitudes, in particular, exhibit negative insolation anomalies from November through March and positive anomalies from June to October (Rojas and Moreno, 2011). We expect that these orbital/insolation differences had a major impact on the glacial extent and especially in the equilibrium line altitudes (ELA) of glaciers. The equilibrium line is a climate sensitive parameter marking the location on a glacier where accumulation of snow is exactly balanced by ablation (net mass balance equals zero) (Porter, 1975). Fluctuations of ELA have been extensively used in paleoclimatic reconstructions because the ELA is primarily controlled by temperature and precipitation (Porter, 1975; Sagredo et al., 2014). In this paper, we explore the differences in the estimated regional ELA between the mid-Holocene (MH, hereafter) and the pre-industrial (PI, hereafter) conditions, based on PMIP2 climate models output in

CPD
11, 603–636, 2015

the Southern Alps in New Zealand and Patagonian Andes in South America (Fig. 1). We hope to answer the question "To what degree was orbital forcing responsible for the larger MH glacier extents apparent from moraine records in Patagonia and the Southern Alps of New Zealand?".

2 Data and methods

2.1 Glacier mass balance model

A simple glacial mass balance model was used to explore the regional differences in the equilibrium line altitudes between the MH and the PI in the southern mid-latitudes. Details of this model can be found in Anderson et al. (2006) and are briefly described here. This model calculates the mass balance gradient for any specific location, based on daily data of temperature and precipitation as a function of elevation. Elevation in the model is defined from 0 to 4000 m a.s.l. with steps of 20 m. For each elevation, the mass balance is calculated based on:

$$\dot{m}(t,z) = \dot{c}(t,z) + \dot{a}(t,z) \tag{1}$$

Where $\dot{m}$ is the mass balance rate, $\dot{c}$ the accumulation rate and $\dot{a}$ the ablation rate at time t and elevation z.

In this model, accumulation is defined as the portion of the daily precipitation that falls as snow when the daily average temperature is below certain temperature threshold (T_{crit}). Previous studies have considered T_{crit} being in the range of 0 to 2 °C (Radic and Hock, 2011). Therefore, water equivalent (w.e.) accumulation is calculated based on the daily information of mean temperature (T_{mean}) and total daily precipitation (p_{d}), and calculated as:

$$c(t,z) = \delta_m p_{\text{d}} \begin{cases} \delta_m = 1, & T_{\text{mean}} < T_{\text{crit}} \\ \delta_m = 0, & T_{\text{mean}} \geq T_{\text{crit}} \end{cases} \tag{2}$$

CPD
11, 603–636, 2015

In this case, T_{crit} was assumed as 1 °C (Anderson et al., 2006).

At mid-latitudes the ablation process is mainly controlled by melting (Rupper and Roe, 2008). Temperature is a good predictor of melt because incoming longwave radiation, and turbulent heat fluxes are important terms in the energy balance that are closely related to air temperature (Ohmura, 2001; Oerlemans, 2001). The other major component of the energy balance, shortwave radiation, is also closely correlated to air temperature.

Ablation is proportional to the mean daily temperature, and occurs for values above 0 °C (Braithwaite, 1985; Hock, 2005). In this study, we calculated ablation using T_{mean} when this is positive:

$$T_d^+(t,z) = \begin{cases} (T_{mean}(t,z) - 0), & T_{mean} > 0\,^\circ\mathrm{C} \\ 0, & T_{mean} \leq 0\,^\circ\mathrm{C} \end{cases} \tag{3}$$

Where T_d^+ is a positive daily temperature.

Ablation is calculated by multiplying the T_d^+ by a factor that relates temperature and ablation, the degree day factor (DDF). The DDF (mm w.e. $d^{-1}\,K^{-1}$) corresponds to the amount of melting (of ice and snow) per day, which occurs when temperatures are higher than 0 °C. This parameter shows great spatial variability and, in general, is higher for ice and lower for snow due to the high albedo of the latter that reduces the available energy for melting (Braithwaite, 1995). In this study we used values of 6 and 3 mm w.e. $d^{-1}\,K^{-1}$ for ice and snow, respectively. These values correspond to the same values used by Woo and Fitzharris (1992) for reconstructing the mass balance for Franz Josef glacier in the Southern Alps. Therefore ablation is estimated by the following relationship:

$$a(t,z) = \mathrm{DDF}_{ice/snow} \cdot T_d^+(t,z) \tag{4}$$

In this study, we use a DDF_{snow} when the snow depth is greater than zero, and DDF_{ice} when the snow depth is equal to zero.

CPD
11, 603–636, 2015

Note that, in this study, we assume that temperatures below zero do not contribute to melting (Hock, 2003), and any potential contribution of sublimation to the total ablation is neglected because it is likely small compared to melting.

By applyng this model at differente elevations, we obtain a glacier mass balance curve, and thus an ELA.

For the purpose of this study we assumed that some parameters such as temperature and precipitation lapse rates, DDFs and temperature threshold T_{crit}, are constant and equal for both the MH and the PI. In this sense, although the absolute value of modelled ELA may not be completely accurate, we are interested in the relative differences between the two periods. The regional differences in ELA between the MH and the PI are still meaningful, given the uncertainties of the chosen parameters (Rupper et al., 2009).

This model has been previously applied to Franz Josef glacier, in New Zealand's Southern Alps, using present-day meteorological data (Anderson et al., 2006).

2.2 Model inputs: PMIP2

As mentioned above, the mass balance model requires daily temperature and precipitation data as inputs. This information was obtained from simulations carried out under the Paleoclimate Modelling Intercomparison Project 2 (PMIP2), see Braconnot et al. (2007) for model setup and boundary conditions. Although PMIP is currently in its third phase (PMIP3) we used the modelling outputs of PMIP2 given that daily data were not available for the most recent phase when this study began. We analysed 7 models of the PMIP2 initiative (Table 1).

The glacier mass balance model was driven for 50 years to be able to capture the inter-annual variability, with daily temperature and precipitation data from the MH and PI experiments. For the validation of the PI climate (Sect. 3.1), and the MH–PI climate differences (Sect. 3.2), we used monthly PMIP2 files.

Temperature data was calculated for different elevations using a standard lapse rate of 6.5 °C km^{-1}. Due to the scarcity of available precipitation observations at high alti-

CPD
11, 603–636, 2015

tude, especially in Patagonia (Garreaud et al., 2013), precipitation was corrected using an observed gradient (in $\mathrm{mm\,m^{-1}}$) in both regions. The observed gradient was obtained using latitudinal and altitudinal distributions of climate station data in both regions. Fitting the precipitation vs. altitude distribution yielded a mean value of $0.00252\,\mathrm{mm\,m^{-1}}$ in Patagonia and $0.0038\,\mathrm{mm\,m^{-1}}$ in New Zealand. In addition a constant precipitation factor (of 1.55) was also applied to account for the underestimation of global precipitation models at high elevations.

The results were averaged over 6 study zones. These zones correspond to: the Chilean Lake District (CLD, approximately between 40–43° S), Northern Patagonian Icefield (NPI, between 43–48° S), Southern Patagonian Icefield (SPI, between 48–53° S) and Cordillera Darwin (CD, between 54–55° S) in South America, and the northern and southern sector of the South Island of New Zealand (NZN, between 41.5–43.5° S; and NZS, 43.5–46° S, respectively) (Fig. 1). We calculated climate differences between MH and PI over these 6 zones, and tested their significance using a t test in the case of temperature, and a non-parametric Wilcoxon–Mann–Whitney test in the case of precipitation with a significance level of 95 %.

We compared the PI outputs with gridded temperature and precipitation data from CRU TS3.10 and CRU TS3.10.01 (CRU hereafter), respectively, to assess the climate model results. CRU is a 0.5° latitude/longitude resolution datasets of mean monthly surface climate over global land areas, excluding Antarctica, which are based on data provided by more than 4000 weather stations for the period 1901 to 2009 (Harris et al., 2014).

In addition, we compared the PI model outputs with meteorological data of stations from both Patagonia and New Zealand (from the Chilean and Argentinean Meteorological Service, and the National Institute of Water and Atmospheric Research, NIWA, respectively).

3 Results

3.1 Model Inputs: validation of PMIP2 outputs

We compared the annual cycle of temperature and precipitation of the PI simulations with the CRU data over the 6 zones of interest (Fig. 1). Given that we are using the PI simulations to evaluate the climate, we compared against the complete 20th century observations. CRU data were averaged over the 1901–2009 period.

Comparison of the annual cycle of monthly temperature between PMIP2 model output and CRU climatological data (Fig. 2) shows that the models are able to reproduce the seasonality and absolute values of the CRU temperature data from the South American sector. The FOAM model, with a very coarse spatial resolution, is the one that exhibits the largest offsets in terms of absolute values. Although the models are able to capture the CRU temperature annual cycle in the New Zealand sectors, they cannot reproduce the absolute temperature values, which are somehow non-systematically offset. Once again, the FOAM model is the one with the lowest performance. Note that some of discrepancies observed can be due to the fact that we are comparing 20th Century climate data with PI climate simulations. Figure 3 shows a longitudinal cross section at 41.1° S (Patagonia) and 43.3° S (South Island, New Zealand), with the models and station climate data. In both regions, but especially in New Zealand, the models do not capture the full longitudinal variations in temperatures. We suggest that, despite its elevation, due to the narrow width of the Southern Alps, the coarse resolution models are not able to capture the impact of this topographic barrier in their temperature estimation.

Annual precipitation cycle (Fig. 4) shows that models have more difficulties at reproducing the present-day monthly precipitation derived from the CRU data, compared with temperature. In general terms, all PMIP2 models reproduce the present-day monthly precipitation in the Chilean Lake District and Northern Patagonian Icefield zones. Precipitation is overestimated in the Southern Patagonian Icefield and Cordillera Darwin sectors. In the case of New Zealand, precipitation is underestimated in both

CPD
11, 603–636, 2015

zones fairly well. Despite this, overall, all models are able to reproduce the seasonality of precipitation.

Figure 5 shows a longitudinal cross section of annual mean precipitation. Once again, the PMIP2 models are not able to simulate longitudinal precipitation gradients over the narrow Southern Alps.

3.2 Climate differences between the mid-Holocene and the pre-industrial

Seasonal temperature differences between the MH and the PI (Fig. 6) shows that most models are consistent, showing temperature anomalies pointing in the same direction and small inter-model spread. Overall, in Patagonia, the models simulate colder conditions during the MH in the austral summer (DJF), austral autumn (MAM) and austral winter (JJA), with average temperature anomalies of ~ -0.2, ~ -0.5 and $\sim -0.4\,^{\circ}$C, respectively. During spring (SON) the PMIP models shows temperatures 0.2 °C warmer.

In New Zealand (Fig. 6) the models show colder MH condition in autumn ($\sim -0.7\,^{\circ}$C) and winter ($\sim -0.4\,^{\circ}$C), and warmer conditions in spring ($\sim 0.3\,^{\circ}$C). In summer the intermodel spread is larger, so that on average, the temperature anomalies are not significant. In the annual mean, the temperature anomalies for South America and New Zealand are identical ($\sim -0.2\,^{\circ}$C).

Estimates of precipitation change show less consistency than for temperatures (Fig. 7), in several cases the models show precipitation anomalies of different sign within regions. Nevertheless, there are some regions and seasons for which the models show consistent precipitation changes. For example, during austral summer and autumn the models suggest that the climate was wetter during the MH compared to PI, in the CLD and the Patagonian Icefields. In general all zones exhibit drier winters than the PI; austral spring was drier in the CLD and NPI, somewhat wetter in the SPI and CD and marginally drier in the New Zealand zones. We find that the CLD was wetter in austral summer and austral autumn, no change in austral winter and dryer in austral spring. Note that none of the precipitation changes are statistically significant.

CPD
11, 603–636, 2015

3.3 ELA calculations

Next we calculated the Equilibrium Line Altitudes over the 6 study zones (Figs. 8 and 9).

We excluded the FOAM model due to its unsatisfactory simulation of the PI climate. The spatial distribution of the PI mean ELA based on six PMIP2 models in Patagonia (Fig. 8), shows, as expected, that the ELA values are higher in the northern section of the study area, with maximum values above 2000 m a.s.l. (mean value of 1797 m a.s.l.) in the CLD. To the south, the ELA decreases gradually, reaching altitudes below 1000 m a.s.l. in SPI (mean value of 956 m a.s.l.) and CD (mean value of 839 m a.s.l., see Table 2). Our results also show that, in general, the inter-model variability (one SD) of the ELA estimation is small. One exception is the inter-model variability observed in the SPI, where the maximum SD is 250 m (mean value of 140 m), in a region with mean ELA of about 950 m a.s.l.

ELA estimates in New Zealand (Fig. 9) are higher in the northern part of South Island (maximum values around 1800 m a.s.l.), and slowly decrease to values of 1400 m a.s.l. at the southern tip of South Island (Table 2). These values show an approximately 200–400 m offset (too high) in absolute terms, compared with observed values (e.g. Chinn et al., 2005). The intermodel spread evaluated with the SD is small in the northern part (148 m). South of 43° S, the intermodel spread becomes larger, with values between 150–180 m on the western flank and up to 200 m on the eastern flank of the Southern Alps. The mean value in this zone is 1528 m a.s.l. (Table 2).

As for the multi model mean ELA differences, in Patagonia (Fig. 10) and in the Southern Alps (Fig. 10) the ELA was lower during the MH compared to PI, however the magnitude of change is relatively small: in Patagonia the mean difference is ∼ 20 m in all zones, in the Southern Alps is ∼ 30 m in both zones. Besides the small estimated ELA variations, it is important to highlight the consistency between ELA differences calculated based on the different PMIP2 model outputs. In the Southern Alps, all of the six models indicate a negative sign in the ELA differences between the MH and the PI (Fig. 10). In Patagonia at least four models show negative differences between MH and

CPD
11, 603–636, 2015

Modelled glacier equilibrium line altitudes during the mid-Holocene

C. Bravo et al.

the PI in almost the entire domain, with five models showing a lower ELA during the MH in some parts of the CLD and SPI zones and six models showing the same result in the west coast of the SPI zone (Fig. 10).

Given these small differences in ELA we performed sensitivity experiments to assess the impact of the value of the precipitation lapse rate on modelled ELA. The sensitivity runs where performed only for Patagonia, because the intermodel spread is largest relative to New Zealand. The values of precipitation lapse-rate are 0, 0.00252, 0.01 and 0.02. These values were chosen in order to sample around the empirical value obtained from the observed precipitation gradient (0.00252 mm m^{-1}).

From the six models used, five models indicate that the MH lower ELA is a robust result, as shown by the estimation performed using the four precipitation lapse rates used in the mass balance model. Moreover, for higher precipitation lapse rates values, the MH ELA becomes lower, increasing the ELA differences between the two periods. We therefore conclude that the small ELA differences in Patagonia are significant and robust to this parameter.

4 Discussion

4.1 Difference between mid-Holocene and pre-industrial climates

In Rojas and Moreno (2011) the full PMIP2 MH simulations were evaluated for the climatic conditions in Patagonia and New Zealand. They found that both regions received less precipitation during a colder accumulation season, and more precipitation during a warmer ablation season. Therefore they suggested, on a qualitative basis, that the temperature and precipitation anomalies could effectively lead to Neoglacial advances.

Our paper goes a step further towards understanding the effects of climatic conditions on glaciers and neoglaciations, and used those conditions to drive a glacier mass balance model.

With respect to the climatic conditions, first of all we notice that the differences in temperatures found in this study are similar to those determined by Ackerley and Renwick (2010) for New Zealand, as well as Rojas and Moreno (2011). Both studies analyzed data from PMIP2 model, but used a different subset of models. Ackerley et al. (2013) use a regional simulation (with corresponding higher spatial resolution) to simulate the MH, and also find a similar temperature pattern. Given that all these studies determine a cooling during the MH with respect to the PI in the autumn months and a warming in the spring months, we conclude that the temperature signals are robust across different subset of PMIP2 simulations for the MH.

With respect to precipitation, in South America, this study indicates mostly wetter conditions during summer (DJF) and drier condition in winter (JJA), in accordance with Rojas and Moreno (2011). For the autumn (MAM) and spring (SON) seasons there is dipole-like signal, with positive precipitation anomalies in the northern regions and drier conditions in the southern regions in MAM and the opposite for SON. These results are also in fair accordance with Rojas and Moreno (2011). For New Zealand the other seasons show large inter-model spread, except during JJA where we find a clear dry condition. Precipitation changes are slightly different than those shown in Ackerly and Renwick (2010), which in turn do not agree with Rojas and Moreno (2011) results. In summary, we find small changes in precipitation and large inter-modal spread, so that existing studies discussed here give slightly different results.

4.2 Differences between mid-Holocene and pre-industrial ELAs

We observed that the mass balance model applied to Patagonia and New Zealand is able to capture the expected differences in the climatological ELA associated with the climate conditions estimated for the MH and the PI (e.g. Rojas and Moreno, 2011; Ackerley and Renwick, 2010). Our results show that during the MH the ELA may have been between 20–30 m lower than the PI times in both Patagonia and New Zealand.

We propose that the results of the modelled ELA differences can be explained mainly by the significant and consistent differences in temperature observed between both pe-

CPD
11, 603–636, 2015

riods, as precipitation differences are more variable. This suggestion is consistent with the idea that glaciers from mid-latitudes are more sensitive to temperature than to precipitation (Anderson and Mackintosh, 2006). Moreover, we suggest that the observed differences of climatological ELA are principally related to the changes in the annual cycle of temperature in these temperate glacier regions. In Patagonia ablation dominantly occurs between September and March (spring and summer months); whereas accumulation occurs from April to August (autumn and winter months) (Rodbell et al., 2009). In New Zealand most of the ablation occurs between November and April (summer and parts of spring and autumn), whereas accumulation occurs from May to October (winter and parts of autumn and spring).

In Patagonia and New Zealand the lower summer temperatures observed during the MH imply less energy input and hence lower amounts of melting. Although the opposite happens in spring, where the higher temperatures of the MH indicate greater melting, we suggest that this change was not sufficient to balance the impact of the lower summer temperature on the mass balance. In addition, the lower temperatures observed during autumn and winter would increase the percentage of precipitation falling as snow rather than rain during the MH, as suggested by Sagredo and Lowell (2012) and Rodbell et al. (2009). This is particularly critical in the Southern Alps, where at present a significant portion of the precipitation falls roughly at the elevation of the ELA, constituting a snow resource if cooling occurs (Rother and Shulmeister, 2006). This can be especially important in autumn and spring, when temperatures in the vicinity of the ELA are typically -1 to $2\,^{\circ}$C. Additionally precipitation during winter is higher during the MH in almost all the PMIP2 models in all zones (Fig. 7), this also contributes to accumulation and therefore a lower ELA in the MH with respect to PI. In Patagonia, where the ELA results showed more spatial variations, sensitivity experiments using the precipitation lapse rates, indicated that when lapse rate value used is bigger the MH ELA value is lower. Given that we have little empirical information to constrain this parameter in Patagonia, the results presented in this study correspond to a lower limit, giving the smallest ELA differences, and therefore represent to most conservative modelled ELA differences.

4.3 Geomorphic evidence of mid-Holocene glacier expansion

As discussed in the introduction, geomorphic and chronological evidence support the idea that glaciers were more extensive during some time of the MH than in the PI and present. Although an exact comparison between our modelling at MH (6000 yr BP) with timing of glacier advances is not possible a couple of example is given below. In Lago General Carrera (named Lago Buenos Aires in the Argentinean side, ~ 46°30′ S), central Patagonia, it has been shown that glaciers advanced around 6200 yr BP (Douglass et al., 2005). Geomorphic evidence at this site suggests that during this glacial advance the ELA dropped to 1100 m a.s.l., a 300 m difference with respect to the present position estimate for small isolated cirque glaciers. Further evidence of glacier activity is found by Harrison et al. (2012) who determined ages of 5700 yr BP for a moraine located to the west of the North Patagonian Icefield (46°36′ S/73°57′ W) associated with San Rafael glacier.

Recently Strelin et al. (2014) found evidence for glacier advance between 6000–5000 yr BP based in moraine dating in the east side of Southern Patagonia Icefield (Lago Argentino), specifically associated with the Upsala, Agassiz and Frías glaciers.

In the Southern Alps, geomorphic and geochronological evidence suggest that Tasman and Mueller glaciers (43°50′ S/170° E) advanced around 6740 ± 160 yr BP (Schaefer et al., 2009, age updated in Putnam et al., 2012). Putnam et al. (2012) estimate for a MH glacial advance at Cameron glacier (~ 43°20′ S/171° E) at 6890 ± 190 yr BP, suggesting a regional event. In Putnam et al. (2012), ELA estimated for MH was ~ 140 m lower than present, and 110 m lower than present 180 ± 48 years ago. This suggests a fairly modest change (~ 30 m) between the MH and PI, consistent with the results of the ELA modelling in this work.

CPD
11, 603–636, 2015

4.4 Comparison of geomorphically-reconstructed ELA and model results

There are few data points to compare the output of the glacier model against reconstructed MH ELAs. While there is a systematic difference between the PI ELA calculated by the model and modern observations, it is clear that relative changes in ELA are very similar between our work and Putnam et al. (2012).

The qualitative agreement in the direction of change between our modeling results and geomorphological reconstructions in these regions, despite absolute differences that are significantly smaller (in the order of the tens of meters), makes us conclude that the mass balance modeling accounts for some but not all of the climatic differences between this two periods.

There are a number of reasons why we do not expect a more quantitative agreement in the absolute value of the ELA. First of all, because of modeling data availability, this study used MH and PI conditions, which are different from late 20th century climatic conditions, for which the reconstructions are compared with, and the fact that we are comparing glacier fluctuations spread throughout the mid-Holocene with a precise time-slice, namely 6 ka BP, in addition to the already discussed uncertainties in the timing of glacial fluctuations. Second the spatial scale of individual glaciers and the coarse resolution of climate models also hinder a direct comparison. Thirdly there are a number of uncertainties in model parameters, especially those related with the spatial distribution of precipitation and degree day factors.

The magnitude of the glacier expansion from a given ELA change depends on local conditions and characteristics of the glaciers, for example, glacier hypsometry. Glacier bed slope is a primary control on length sensitivity (Oerlemans, 2012) where a glacier with a gentle bed slope, such as Upsala Glacier, shows a high length sensitivity to ELA changes, estimated at ~ -50 m of glacier length per metre of ELA increase (Oerlemans, 2012) with large change of the accumulation and ablation areas even if the ELA oscillation is small (Mercer, 1965; Furbish and Andrews, 1984). In contrast, the steep Franz Josef Glacier shows a much smaller length sensitivity of ~ -10 (dimensionless).

CPD
11, 603–636, 2015

Other parameters not considered in this study are surface debris cover (Anderson and Mackintosh, 2012), and iceberg calving (Koppes et al., 2011).

Considering all these aspects and limitations of the glacier mass balance model, we highlight this qualitative agreement in both the sign of change and regional homogeneity within and between both study regions. This in-phase ELA response in Patagonia and New Zealand's South Island, is also in agreement with the glaciers fluctuations observed during the 20th century in Patagonia and the Southern Alps, where glaciers seem to be in phase to similar climate forcing (Fitzharris et al., 2007).

5 Conclusions

A glacier mass balance model forced with PMIP2 simulations showed that southern mid-latitude glacier ELAs during the mid-Holocene(MH) were lower compared to pre-industrial (PI) conditions. The fact that the ELA differences had the same sign in the two time slices, and in all the models used in New Zealand's South Island and in most of the models in Patagonia, gives confidence in the obtained results. The main forcing of the modelled ELA differences are temperature differences resulting from changing insolation at the top of the atmosphere. Significantly colder conditions during the summer, autumn and winter months prevailed during the MH compared to the PI. These temperature changes were driven by orbitally controlled insolation variations. In contrast, modelled precipitation changes were small and less robustly simulated, indicating a slight annual increase. Our ELA results for the MH underline the evidence that temperate glaciers show a greater sensitivity to temperature changes than changes in precipitation (Anderson and Mackintosh, 2006).

Temperature changes cause a double effect in glacier mass balance. First, in summer and early autumn in the MH, less energy is available for melting and second, from autumn to late winter, lower temperatures cause a larger portion of precipitation to fall as snow, resulting in higher accumulation in the MH with respect to the PI, as well as

CPD
11, 603–636, 2015

a higher surface albedo which reduces the amount of short-wave radiation available for melt.

Coming back to our initial question expressed in the introduction, this study provides new insights towards understanding mid-Holocene glacier conditions, demonstrating that orbital forcing is consistent with a hemispheric pattern of larger glacier extent at MH.

There is qualitative agreement between our modelling results, and ELA reconstructions based on geomorphic and geochronologic evidence, which shows that glaciers in both Patagonia and New Zealand exhibited a lower ELA during the MH than in PI times.

Acknowledgements. We acknowledge the international modelling groups for providing their data for analysis, the Laboratoire des Sciences du Climatet de l'Environnement (LSCE) for collecting and archiving the model data. The PMIP2/MOTIF Data Archive is supported by CEA, CNRS, the EU project MOTIF (EVK2-CT-2002-00153) and the Programme National d'Etude de la Dynamique du Climat (PNEDC). C. Bravo acknowledges the support of CONICYT magister scholarship. The Millennium Nucleus NC120066 and CR2 N15110009 supported this investigation. M. Rojas and P. I. Moreno received support by FONDECYT grant # 1131055. E. Sagredo acknowledges support by FONDECYT Iniciación Grant # 11121280 and CONICYT Grant USA-2013-0035. A. N. Mackintosh and B. M. Anderson acknowledge financial support from Victoria University Foundation Grant, "Antarctic Research Centre Climate and Ice-Sheet Modelling".

References

Ackerley, D. and Renwick, J. A.: The Southern Hemisphere semiannual oscillation and circulation variability during the Mid-Holocene, Clim. Past, 6, 415–430, doi:10.5194/cp-6-415-2010, 2010.

Ackerley, D., Lorrey, A., Renwick, J., Phipps, S., Wagner, S., and Fowler, A.: High resolution modelling of mid-Holocene New Zealand climate at 6000 yr BP, Holocene, 23, 1272–1285, 2013.

Anderson, B. and Mackintosh, A.: Temperature change is the major driver of late-glacial and Holocene glacier fluctuations in New Zealand, Geology, 34, 121–124, 2006.

Anderson, B. and Mackintosh, A.: Controls on mass balance sensitivity of maritime glaciers in the Southern Alps, New Zealand: the role of debris cover, J. Geophys. Res., 117, F01003, doi:10.1029/2011JF002064, 2012.
Anderson, B., Lawson, W., Owen, I., and Goodsell, B.: Past and future mass balance of "Ka Roimata o Hine Hukatere" Franz Josef Glacier, New Zealand, J. Glaciol., 52, 597–607, 2006.
Aniya, M.: Holocene glacial chronology in Patagonia: Tyndall and Upsala glaciers, Arctic Alpine Res., 27, 311–322, 1995.
Aniya, M.: Holocene glaciations of Hielo Patagónico (Patagonia Icefiled), South America: a brief review, Geochem. Rev., 47, 97–105, 2013.
Braconnot, P., Otto-Bliesner, B., Harrison, S., Joussaume, S., Peterchmitt, J.-Y., Abe-Ouchi, A., Crucifix, M., Driesschaert, E., Fichefet, Th., Hewitt, C. D., Kageyama, M., Kitoh, A., Laîné, A., Loutre, M.-F., Marti, O., Merkel, U., Ramstein, G., Valdes, P., Weber, S. L., Yu, Y., and Zhao, Y.: Results of PMIP2 coupled simulations of the Mid-Holocene and Last Glacial Maximum – Part 1: experiments and large-scale features, Clim. Past, 3, 261–277, doi:10.5194/cp-3-261-2007, 2007.
Braithwaite, R.: Calculation of degree-days for glacier–climate research, Z. Gletscherkunde Glazialgeologie, 20, 1–8, 1985.
Braithwaite, R.: Positive degree-day factors for ablation on the Greenland ice sheet studied by energy-balance modelling, J. Glaciol., 41, 153–160, 1995.
Chinn, T., Heydenrych, C., and Salinger, M. J.: Use of ELA as a practical method of monitoring glacier response to climate in New Zealand's Southern Alps, J. Glaciol., 51, 85–95, 2005.
Clapperton, C. and Sugden, D.: Holocene glacier fluctuations in South America and Antarctica, Quaternary Sci. Rev., 7, 185–198, 1988.
Douglass, D., Singer, B., Kaplan, M., Ackert, R., Mickelson, D., and Caffe, M.: Evidence of early Holocene glacial advances in southern South America from cosmogenic surface-exposure dating, Geology, 33, 237–240, 2005.
Fitzharris, B., Clare, G., and Renwick, J.: Teleconnections between Andean and New Zealand glaciers, Global Planet. Change, 59, 159–174, 2007.
Fletcher, M. and Moreno, P.: Have the Southern Weterlies changes in a zonally symmetric manner over the last 14 000 years? A hemisphere-wide take on a controversial problem, Quatern. Int., 254, 32–46, 2012.
Furbish, D. and Andrews, J.: The use of hypsometry to indicate long-term stability and response of valley glaciers to changes in mass transfer, J. Glaciol., 30, 192–211, 1984.

CPD
11, 603–636, 2015

Garreaud, R., Lopez, P., Minvielle, M., and Rojas, M.: Large scale control on the Patagonia climate, J. Climate, 26, 215–230, 2013.
Gellatly, A., Chinn, T., and Röthlisberger, F.: Holocene glacier variation in New Zealand: a review, Quaternary Sci. Rev., 7, 227–242, 1988.
Harris, I., Jones, P., Osborn, T., and Lister, D.: Updated high-resolution grids of monthly climatic observations – the CRU TS3.10 Dataset, Int. J. Climatol., 34, 623–642, 2014.
Harrison, S., Glasser, N., Duller, G., and Jansson, K.: Early and mid-Holocene age for the Tempanos Moraine, Laguna San Rafael, Patagonian Chile, Quaternary Sci. Rev., 31, 82–92, 2012.
Hock, R.: Temperature index melt modelling in mountains areas, J. Hydrol., 282, 104–115, 2003.
Hock, R.: Glacier melt: a review of processes and their modeling, Prog. Phys. Geog., 29, 362–391, 2005.
Kaplan, M., Schaefer, J., Denton, G., Doughty, A., Barrel, D., Chinn, T., Putnam, A., Andersen, B., Mackintosh, A., Finkel, R., Schwartz, R., and Anderson, B.: The anatomy of long-term warming since 15 ka in New Zealand based on net glacier snowline rise, Geology, 41, 887–890, doi:10.1130/g34288.1, 2013.
Koppes, M., Conway, H., Rasmussen, L. A., and Chernos, M.: Deriving mass balance and calving variations from reanalysis data and sparse observations, Glaciar San Rafael, northern Patagonia, 1950–2005, The Cryosphere, 5, 791–808, doi:10.5194/tc-5-791-2011, 2011.
Mayewski, P., Rohling, E., Stager, J., Karlén, W., Maasch, K., Meeker, L., Meyerson, E., Gasse, F., Van Kreveld, S., Holmgren, K., Lee-Thorp, J., Rosqvist, G., Rack, F., Staubwasser, M., Schneider, R., and Steig, E.: Holocene climate variability, Quaternary Res., 62, 243–255, 2004.
Mercer, J.: Glacier variations in southern Patagonia, Geogr. Rev., 55, 390–413, 1965.
Mercer, J.: Holocene glacier variation in southern South America, Striae, 18, 35–40, 1982.
Moreno, P., Francois, J. P., Villa-Martinez, R., and Moy, C.: Covariability of the Southern Westerlies and atmospheric CO_2 during the Holocene, Geology, 38, 727–730, 2010.
Oerlemans, J.: Glaciers and Climate Change, A. A. Balkema Publisher, Lisse, 2001.
Oerlemans, J.: Linear modelling of glacier length fluctuations, Geogr. Ann. A., 94, 183–194, doi:10.1111/j.1468-0459.2012.00469.x, 2012.
Ohmura, A.: Physical basis for the temperature-based melt-index method, J. Appl. Meteorol., 40, 753–761, 2001.

Porter, S.: Equilibrium line altitudes of late Quaternary glaciers in the Southern Alps, New Zealand, Quaternary Res., 5, 27–47, 1975.
Porter, S.: Onset of neoglaciation in Southern Hemisphere, J. Quaternary Sci., 15, 395–408, 2000.
Porter, S. and Denton, G.: Chronology of neoglaciation in the North American Cordillera, Am. J. Sci., 265, 177–210, 1967.
Putnam, A., Schaefer, J., Denton, G., Barrel, D., Finkel, R., Anderson, B., Schwartz, R., Chinn, T., and Doughty, A.: Regional climate control of glaciers in New Zealand and Europe during the pre-industrial Holocene, Nat. Geosci., 5, 627–630, doi:10.1038/ngeo1548, 2012.
Radic, V. and Hock, R.: Regionally differentiated contribution of mountain glaciers and ice caps to future sea level rise, Nat. Geosci., 4, 91–94, 2011.
Rodbell, D., Smith, J., and Mark. B.: Glaciation in the Andes during Lateglacial and Holocene, Quaternary Sci. Rev., 28, 2165–2212, 2009.
Rojas, M. and Moreno, P.: Atmospheric circulation changes and neoglacial conditions in the Southern Hemisphere mid-latitudes: insights from PMIP2 simulation at 6 kyr, Clim. Dynam., 37, 357–375, 2011.
Rojas, M., Moreno, P., Kageyama, M., Crucifix, M., Hewitt, C., Abe, A., Ohgaito, R., Brady, E., and Hope, P.: The Last Glacial Maximum in the Southern Hemisphere in PMIP2 simulations, Clim. Dynam., 32, 525–548, 2009.
Rother, H. and Shulmeister, J.: Synoptic climate change as a driver of late Quaternary glaciations in the mid-latitudes of the Southern Hemisphere, Clim. Past, 2, 11–19, doi:10.5194/cp-2-11-2006, 2006.
Rupper, S. and Roe, G.: Glacier change and regional climate: a mass and energy balance approach, J. Climate, 21, 5384–5401, 2008
Rupper, S., Roe, G., and Gillespie, A.: Spatial patterns of Holocene glacier advance and retreat in Central Asia, Quaternary Res., 72, 337–346, 2009.
Sagredo, E. and Lowell, T.: Climatology of Andean glaciers: a framework to understand glacier response to climate change, Global Planet. Change, 86–87, 101–109, 2012.
Sagredo, E., Rupper, S., and Lowell, T.: Sensitivities of the equilibrium line altitude to temperature and precipitation changes along the Andes, Quaternary Res., 81, 355–366, 2014.

CPD
11, 603–636, 2015

Schaefer, J., Denton, G., Kaplan, M., Putman, A., Finkel, R., Barrel, D., Anderson, B., Schwartz, R., Mackintosh, A., Chinn, T., and Schluchter, C.: High-frequency Holocene glacier fluctuation in New Zealand differs from the northern signature, Science, 324, 622–625, 2009.
Solomina, O., Bradley, R., Hodgson, D. A., Ivy-Ochs, S., Jomelli, V., Mackintosh, A., Nesje, A., Owen, L., Wanner, H., Wiles, G. C., and Young, N. E.: Holocene glacier fluctuations, Quaternary Sci. Rev., 111, 9–34, 2015.
Strelin, J., Kaplan, M., Vandergoes, M., and Denton, G.: Holocene glacier history of the Lago Argentino basin, Southern Patagonian Icefield, Quaternary Sci. Rev., 101, 124–145, 2014.
Woo, M. and Fitzharris, B. B.: Reconstruction of mass balance variations for Franz Josef Glacier, New Zealand, 1913–1989, Arctic Alpine Res., 24, 281–290, 1992.

CPD
11, 603–636, 2015

Modelled glacier equilibrium line altitudes during the mid-Holocene

C. Bravo et al.

Table 1. PMIP2 models used in this study.

Models	Atmosphere lon × lat	Vertical levels	Years of data used
CSIRO-Mk3L-1.1	5.625 × ~ 3.18	18	50
ECHAM5-MPIOM1	3.75 × 2.5	20	50
FOAM	7.5 × 4.5	18	50
MIROC3.2	2.8 × 2.8	20	50
MRI-CGCM2.3.4fa	2.8 × 2.8	30	50
MRI-CGCM2.3.4nfa	2.8 × 2.8	30	50
UBRIS-HadCM3M2	3.75 × 2.5	19	50

Table 2. Mean values of ELA for each zone.

Region	Zones	ELA MH [m a.s.l.]	ELA PI [m a.s.l.]	Difference [m]
Patagonia	Chilean Lake District	1776 ± 99	1797 ± 93	−21
	Northern Patagonia Icefield	1333 ± 125	1354 ± 106	−21
	Southern Patagonia Icefield	939 ± 148	956 ± 140	−17
	Cordillera Darwin	821 ± 90	839 ± 89	−18
South Island, New Zealand	North	1667 ± 144	1697 ± 148	−30
	South	1501 ± 176	1528 ± 176	−27

CPD
11, 603–636, 2015

Modelled glacier equilibrium line altitudes during the mid-Holocene

C. Bravo et al.

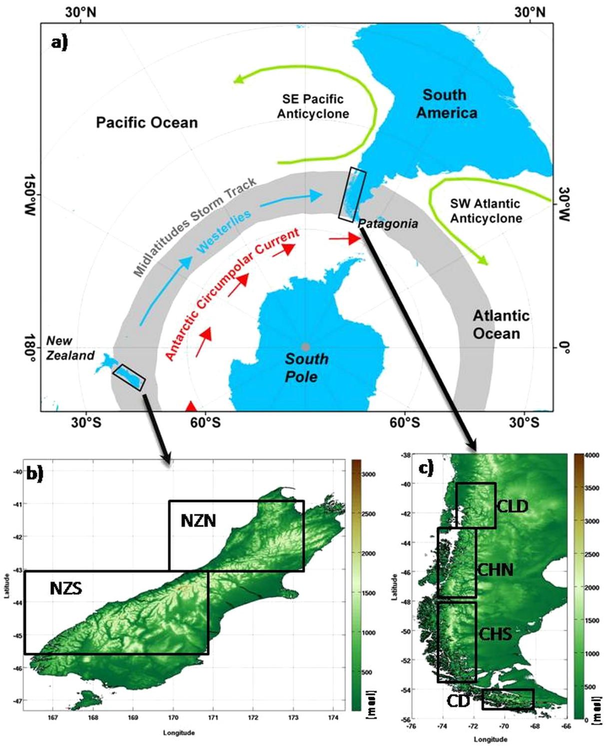

Figure 1. Study area. **(a)** Schematic diagram showing some of the main climate characteristics in the southern mid-latitudes. **(b)** New Zealand southern island topography and the two zones of analysis (NZN: New Zealand north, NZS, and New Zealand south). **(c)** Patagonia topography and the four zones of analysis (CLD: Chilean Lake District, CHN: North Patagonian Icefield, CHS: South Patagonian Icefield and CD: Cordillera Darwin).

CPD
11, 603–636, 2015

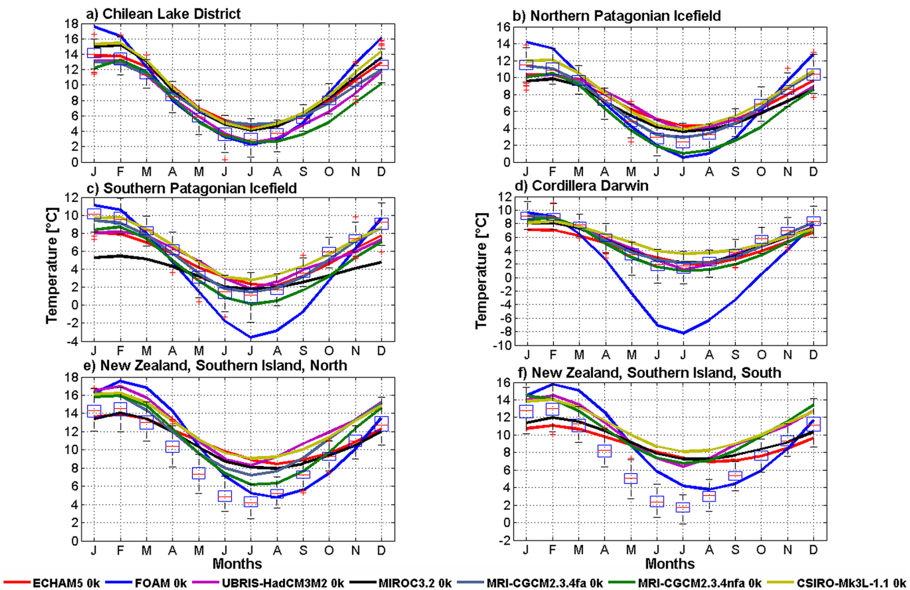

Figure 2. Annual cycle of temperature of six zones. **(a–d)** correspond to Patagonia and (**e** and **f**) correspond to New Zealand. PMIP2-PI simulations (colour lines), CRU temperatures (boxplots), including inter-annual variability.

CPD
11, 603–636, 2015

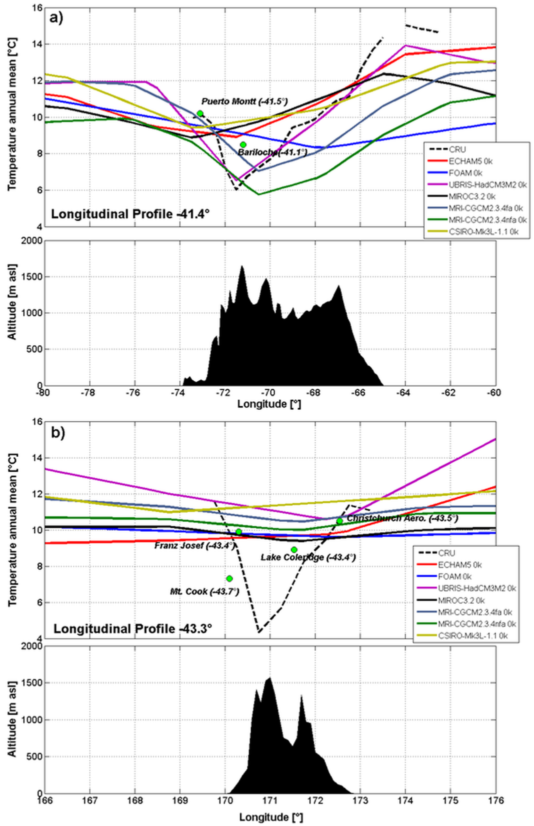

Figure 3. Longitudinal profile showing PMIP2-PI temperature simulations (colour lines) and CRU temperature (dash line). Green points are observed station data. **(a)** Patagonia profile at 41.1° S and **(b)** New Zealand profile at 43.3° S.

CPD
11, 603–636, 2015

Modelled glacier equilibrium line altitudes during the mid-Holocene

C. Bravo et al.

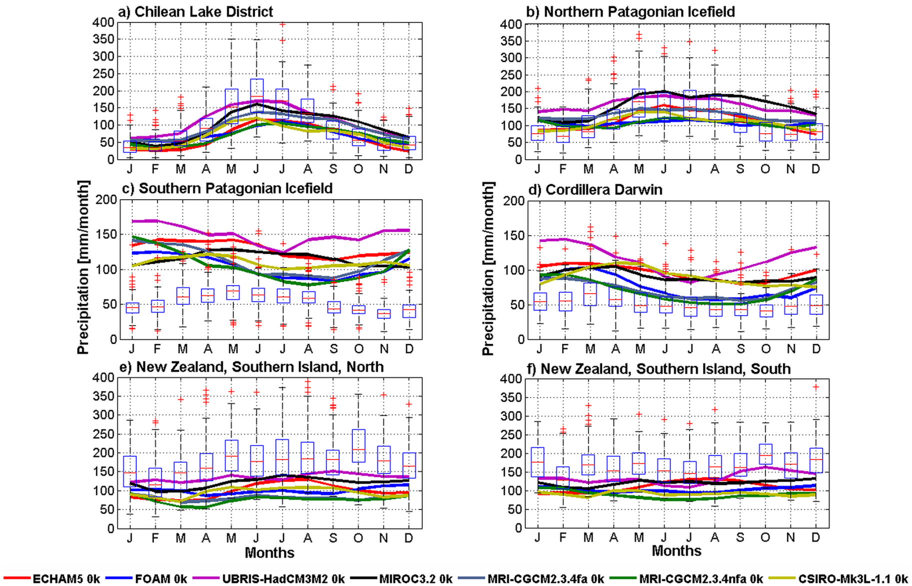

Figure 4. Annual cycle of precipitation of six zones. **(a–d)** correspond to Patagonia and (**e** and **f**) correspond to New Zealand. PMIP2-PI simulations (colour lines), CRU precipitation (boxplots), including inter-annual variability.

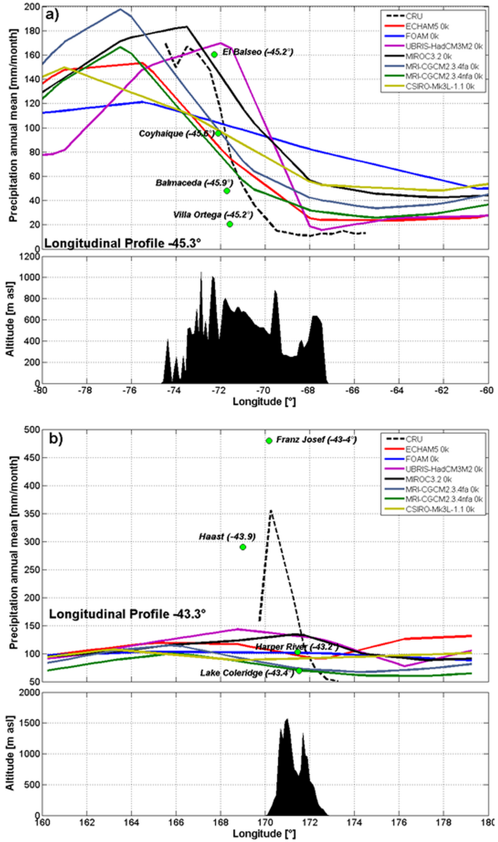

Figure 5. Longitudinal profile showing PMIP2-PI precipitation simulations (colour lines) and CRU precipitation (dash line). Green points are observed station data. **(a)** corresponds to a Patagonia profile at 45.3° S and **(b)** to a New Zealand profile at 43.3° S.

CPD
11, 603–636, 2015

Modelled glacier equilibrium line altitudes during the mid-Holocene

C. Bravo et al.

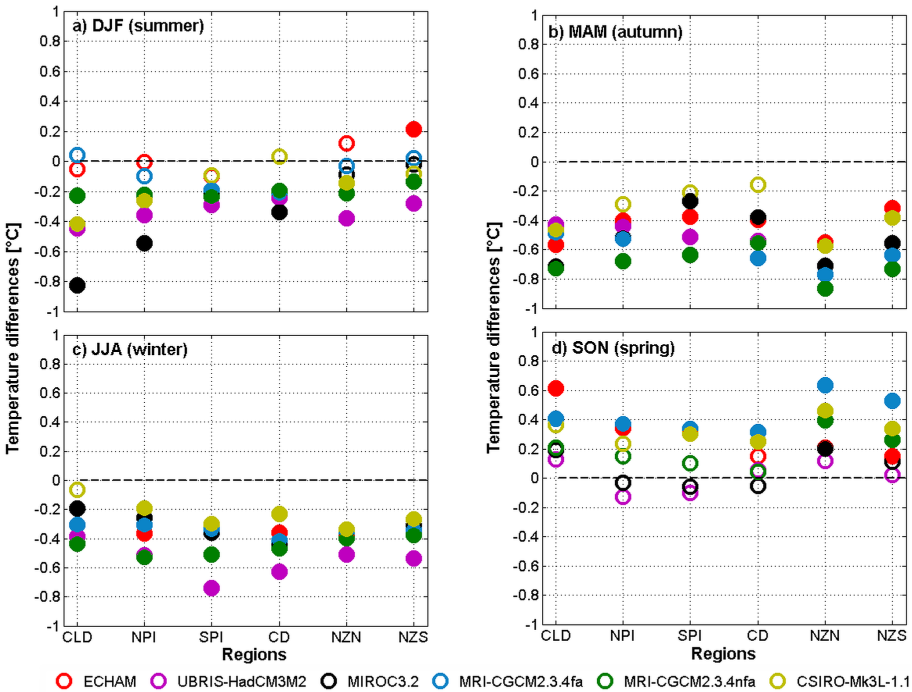

Figure 6. Temperature differences: mid-Holocene minus Preindustrial, over the 6 zones of analysis. **(a)** DJF, **(b)** MAM, **(c)** JJA, **(d)** SON. Filled circles correspond to statistically significant differences ($p \leq 0.05$).

CPD
11, 603–636, 2015

Modelled glacier equilibrium line altitudes during the mid-Holocene

C. Bravo et al.

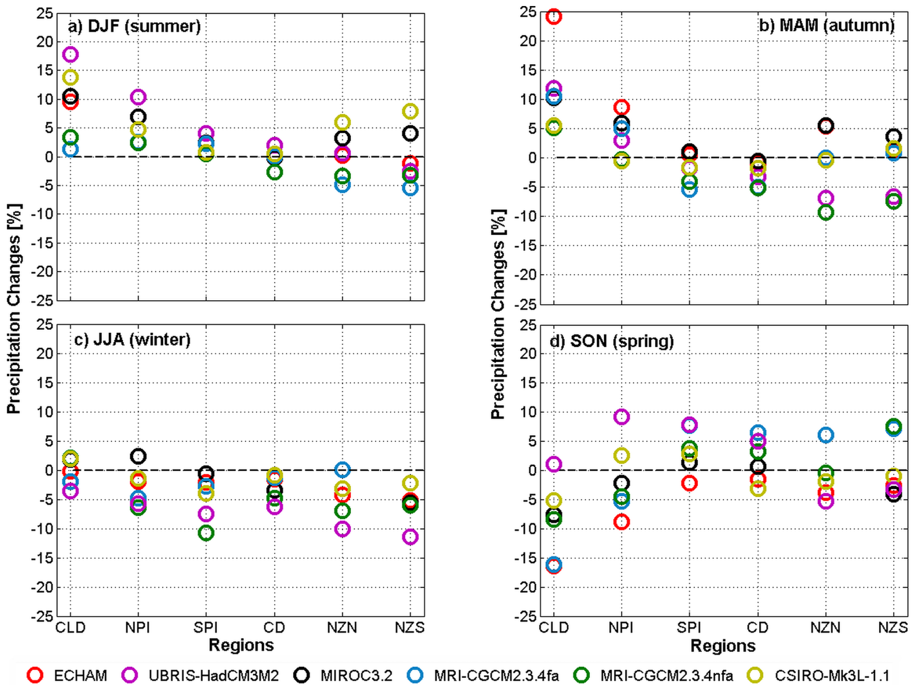

Figure 7. Precipitation differences: mid-Holocene minus Preindustrial, over the 6 zones of analysis. **(a)** DJF, **(b)** MAM, **(c)** JJA, **(d)** SON. Filled circles correspond to statistically significant differences ($p \leq 0.05$).

CPD
11, 603–636, 2015

Modelled glacier equilibrium line altitudes during the mid-Holocene

C. Bravo et al.

Title Page
Abstract | Introduction
Conclusions | References
Tables | Figures
◀| |▶
◀ ▶
Back | Close
Full Screen / Esc
Printer-friendly Version
Interactive Discussion

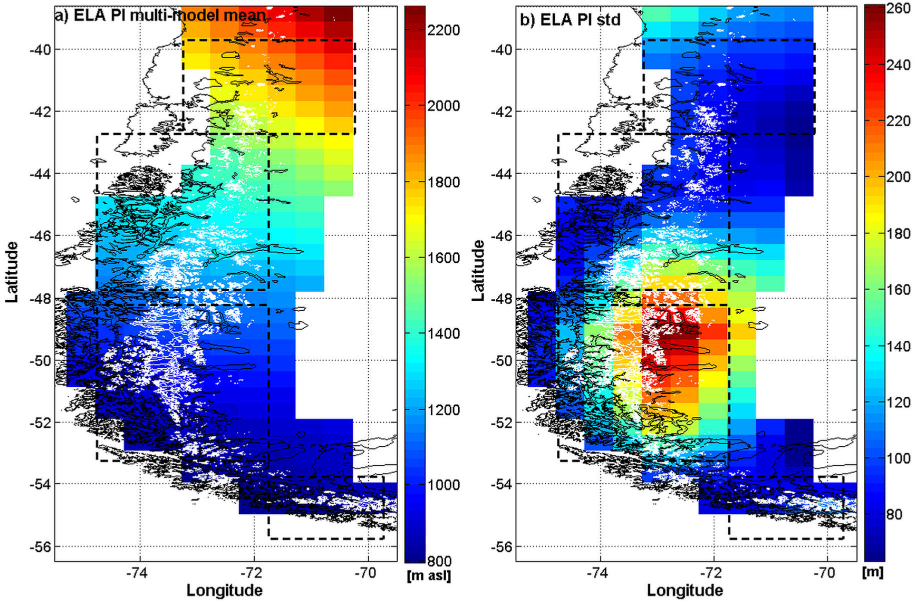

Figure 8. Spatial distribution of pre-industrial equilibrium line altitude (ELA) in South America based on six PMIP2 simulations. **(a)** Mean ELA (m a.s.l.) and **(b)** inter-model variability of the ELA (one SD). White lines correspond to actual glacier extension according to the Randolph Glacier Inventory (RGI 3.2).

CPD
11, 603–636, 2015

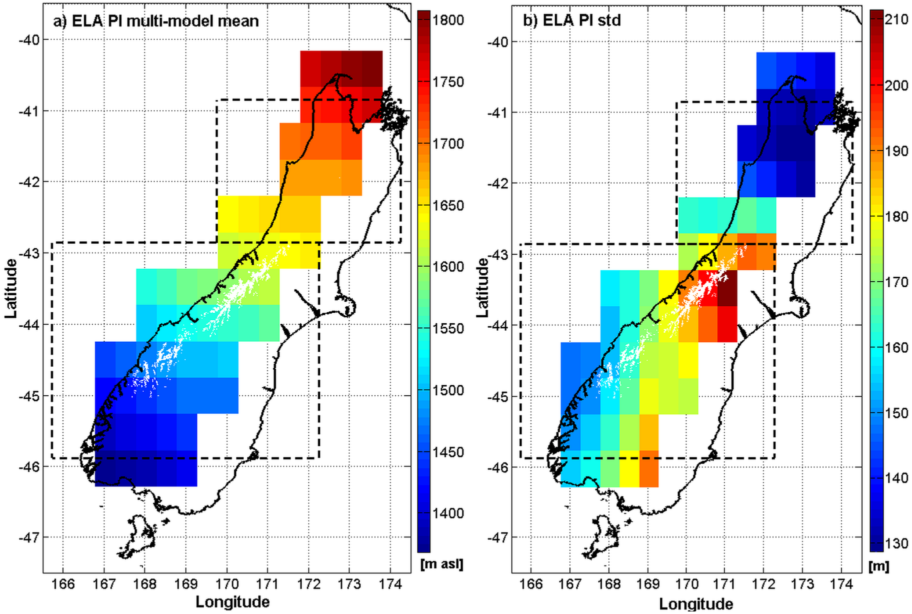

Figure 9. Spatial distribution of pre-industrial equilibrium line altitude (ELA) in Southern Island of New Zealand based on six PMIP2 simulations. **(a)** Mean ELA (m a.s.l.) and **(b)** inter-model variability of the ELA (one SD). White lines correspond to actual glacier extension according to the Randolph Glacier Inventory (RGI 3.2).

CPD
11, 603–636, 2015

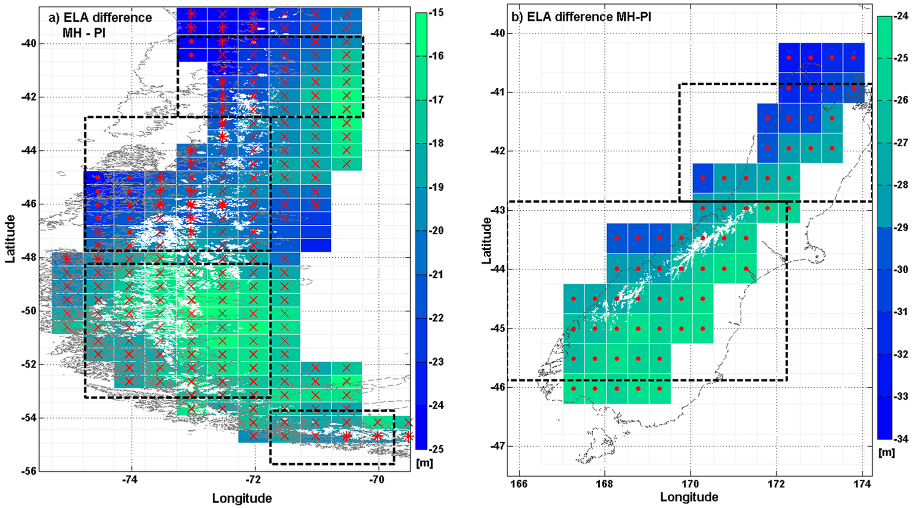

Figure 10. Holocene minus pre-industrial equilibrium line altitude differences. Points indicate that the six models have a negative sign in the differences; asterisks indicate that five models have a negative sign and crosses indicate that four models have a negative sign. White lines indicate actual glacier outlines (Randolph Glacier Inventory 3.2). **(a)** Patagonia, **(b)** New Zealand.

CPD
11, 603–636, 2015